MATERIALS CHEMISTRY FRONTIERS

CCS 中国化学会 CHINESE CHEMICAL SOCIETY

ICCAS

ROYAL SOCIETY OF CHEMISTRY

REVIEW

View Article Online
View Journal | View Issue

Cite this: *Mater. Chem. Front.*, 2021, **5**, 1221

Research and progress of black metastable phase $CsPbI_3$ solar cells

Huanhuan Yao, Jing Zhao, Zhizai Li, Zhipeng Ci * and Zhiwen Jin *

Received 28th September 2020,
Accepted 10th November 2020

DOI: 10.1039/d0qm00756k

rsc.li/frontiers-materials

Recently, all-inorganic perovskite semiconductors have received widespread attention due to their excellent thermal stability. Among them, $CsPbI_3$ with a suitable band gap (<1.73 eV) has achieved a power conversion efficiency (PCE) of more than 19%. However, at room temperature, its black phase easily turns into a yellow non-perovskite phase, which limits its commercial application. Particularly, among the three black phases, the cubic phase usually can be obtained at high temperature, and the preparation conditions are harsh, which limits its development in other regions. On the other hand, the metastable phases (β, γ phase) are relatively stable due to lower dissociation and formation energy, and lower phase transition temperature. Therefore, in this review, we mainly talk about the $CsPbI_3$ perovskite solar cells (PSCs) based on the metastable phase. First, we introduce the crystal structure and electronic structure of the inorganic $CsPbI_3$ perovskite. Then, the reasons for the thermodynamic instability of $CsPbI_3$ are analyzed. Next, we focus on the latest progress in improving the performance and stability of $CsPbI_3$ PSCs based on the metastable phase. Finally, the challenges and prospects for the future development of efficient and stable $CsPbI_3$ perovskite solar cells are proposed.

1. Introduction

The depletion of traditional non-renewable energy sources and global warming caused by the use of these energy sources urgently demand the application of new renewable energy sources. Among them, photovoltaics, as a clean and endless energy source, are drawing people's attention. In 2009, Miyasaka *et al.* first used methylammonium (MA^+) lead triiodide ($MAPbI_3$) as a visible light sensitizer for dye-sensitized solar cells, and achieved a power conversion efficiency (PCE) of 3.8%.[1] After just ten years of development, in 2020, the PCE of perovskite solar cells (PSCs) has increased to 25.5%, which is close to that of the champion silicon solar cells (26.7%), and its growth rate is unprecedented and extremely encouraging.[2–9]

Among various photovoltaic devices, organic–inorganic hybrid PSCs have shown excellent performance. However, due to the hygroscopicity and volatility of organic cations, water, oxygen, light and high temperature can cause chemical instability and make it easy to decompose, and thus seriously hinder their commercial applications.[10–17] In order to solve this problem,

Key Laboratory of Special Function Materials and Structure Design (MoE) & National & Local Joint Engineering Laboratory for Optical Conversion Materials and Technology & School of Physical Science and Technology, Lanzhou University, Lanzhou 730000, China. E-mail: cizhp@lzu.edu.cn, jinzw@lzu.edu.cn

Huanhuan Yao

Huanhuan Yao received her BS degree from the School of Physics and Electronic Engineering, Northwest Normal University. She is currently a MS student at Lanzhou University. Her main research focuses on organic–inorganic hybrid semiconductor materials and solar cells.

Jing Zhao

Jing Zhao received her BS degree from the School of Optoelectronic Engineering, Changzhou Institute of Technology. She is currently a MS student at Lanzhou University. Her main research focuses on inorganic semiconductor materials and solar cells.

the inorganic cesium (Cs) cation is used to replace organic cations to improve stability.[18–23] In the all-inorganic cesium-lead halide perovskite ($CsPbX_3$, X = Cl, Br, I), the cubic phase (α-phase) $CsPbI_3$ has excellent stability, and will not decompose even at a high temperature of 400 °C. In addition, it has the most suitable band gap (<1.73 eV) as the top cells for perovskite/silicon tandem solar cells.[24,25] However, because the radius of Cs^+ is so small that the tolerance factor (t) deviates from the ideal value, α-$CsPbI_3$ usually can be obtained at a high temperature (>320 °C).[26–28] At room temperature (RT), although its quantum dot (QD) structure is thermodynamically stable, its thin film is very unstable that $CsPbI_3$ would spontaneously transform into the non-perovskite yellow phase (δ-$CsPbI_3$).[29–31]

Therefore, how to improve its phase stability has been extensively explored.[32–34] The main strategies are ion doping, introducing metastable phases, developing low-dimensional PSCs, and introducing steric hindrance. In particular, the metastable phases (tetragonal (β) and quadrature (γ)) are more stable than the α phase due to their lower dissociation and formation energy, and lower phase transition temperature.[35–37] However, there are a few summaries on the metastable phase, and most of them are based on the overall $CsPbI_3$. Therefore, in this review, we mainly discuss the research and progress of $CsPbI_3$ PSCs based on the metastable phase. In the first part, we introduce its crystal structure and electronic structure. In the second part, we give the reasons for its thermodynamic instability. The third part focuses on the latest developments in the performance and stability of $CsPbI_3$ PSCs based on the metastable phase. Finally, we give our own opinions on the future development of efficient and stable $CsPbI_3$ PSCs.

2. Crystal/electronic structure

In order to understand the photophysical properties and composition stability of the $CsPbI_3$ semiconductor, we first analyze its crystal structure and electronic structure, starting from the most basic point, and exploring the source of its instability.

2.1 Crystal structure

In the $CsPbX_3$ perovskite structure, Cs^+ occupies the cubic cavity of the $[PbX_6]^{4-}$ octahedron, and the Pb atom fills the octahedral voids.[38] The formation and stability of the perovskite structure are mainly determined by the following parameters: Goldschmidt tolerance factor t and octahedral factor μ:[39,40]

$$t = \frac{r_A + r_X}{\sqrt{2}(r_B + r_X)} \quad (1)$$

$$\mu = \frac{r_B}{r_X} \quad (2)$$

Here r_A, r_B and r_X are the ionic radii of the Cs, Pb and X positions, respectively. Generally, the three-dimensional (3D) perovskite structure is formed when t is 0.8–1, and when t is 0.9–1, a cubic structure can be obtained, as shown in Fig. 1a.[41,42] However, as t decreases below 0.9, the 3D perovskite structure deforms due to the inclination of the octahedron. In addition, when the radius of the A-site cation is too large and $t > 1$ the 3D structure is destroyed. The chemical bonds between the octahedral layers are opened, and large-sized organic cations connect two adjacent octahedra through intermolecular forces to form two-dimensional (2D) PSCs. This causes steric effects by introducing long-chain organic cations to prevent phase change, which is beneficial to improve the

Zhizai Li

Zhizai Li received his BS degree from the School of Physical Science and Technology, Lanzhou University. He is currently a PhD student under the supervision of Prof. Zhiwen Jin. His main research focuses on inorganic semiconductor materials and solar cells.

Zhipeng Ci

Zhipeng Ci is an associate professor of the School of Physical Science and Technology, Lanzhou University. He obtained a BS degree and a PhD degree from Lanzhou University in 2003 and 2010, respectively. Currently he is mainly engaged in the research of low dimensional photoelectric materials and photophysics mechanism.

Zhiwen Jin

Zhiwen Jin received his BS degree from Lanzhou University in 2011 and PhD degree from Institute of Chemistry, Chinese Academy of Sciences in 2016. He joined Lanzhou University in 2018 as a full professor with the School of Physical Science and Technology, Lanzhou University. His research interests include inorganic quantum dots and semiconductor materials, thin-film photoelectric devices and device physics.

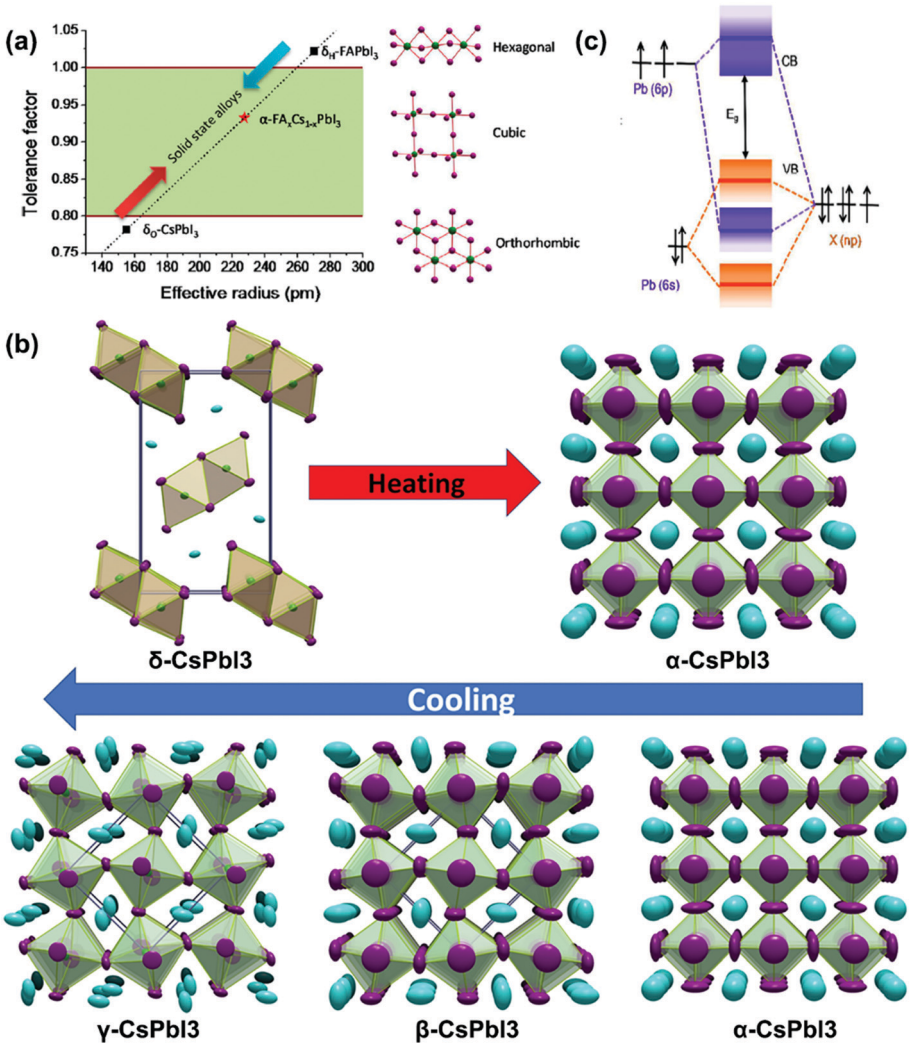

Fig. 1 (a) The relationship between tolerance factor and crystal structure. Reproduced with permission.[41] Copyright 2016, American Chemical Society Publications. (b) The phase transition of the crystal structure in $CsPbI_3$ changes with temperature. Reproduced with permission.[36] Copyright 2018, American Chemical Society Publications. (c) A schematic diagram of $APbX_3$ bonding/antibonding orbitals, showing how the valence band (VB) and conduction band (CB) are formed. Reproduced with permission.[49] Copyright 2016, American Chemical Society Publications.

stability of $CsPbI_3$.[43,44] If the A-site cation is too small and $t < 0.8$, it is not conducive to the formation of the 3D perovskite.

At the same time, for a typical stable 3D perovskite structure, its t should be greater than 0.875 and μ should be greater than 0.41. However, for $CsPbI_3$, the Cs^+ is not large enough to accommodate the $[PbX_6]^{4-}$ octahedron, resulting in a t of approximately 0.8472 and a μ of approximately 0.47. Hence, $CsPbI_3$ shows instable structure.[45] Meanwhile, due to its small t, $CsPbI_3$ tends to be a yellow non-perovskite phase at RT.

For $CsPbI_3$, there are four phases with different structures: cubic (α), tetragonal (β), orthogonal (γ) and non-perovskite phase (δ), as shown in Fig. 1b.[36] Among them, the yellow δ phase is composed of a non-corner-sharing $[PbI_6]^{4-}$ octahedron, while the other three black phases are composed of a corner-sharing $[PbI_6]^{4-}$ octahedron. However, the Pb–I–Pb bond angle (φ) of the three black phases is also different from each other. Specifically, the φ of the cubic phase is 180°. The β phase and γ phase are generated by twisting the bond angle, the φ of which is about 170° and 150°, respectively.[46] In general, the transformation from α phase to β and γ phase is through the distortion of the $[PbI_6]^{4-}$ octahedron without destroying the 3D Pb–I network. Meanwhile, the phase transition of $CsPbI_3$ PSCs is a reversible process. The δ phase transforms into the α phase at high temperature (>350 °C). During the cooling process, it undergoes an α to β phase transition at 260 °C, then transforms to the γ phase at 175 °C. When the γ phase is placed at ambient air, it immediately transforms into the δ phase, which mainly ascribes to its own thermodynamic instability (internal reasons).[36] Besides, when encountering polar solvents (external causes), such as 4-*tert*-butylpyridine (tBP) and ethanol, it also tends to transform into the δ phase.[47,48]

2.2 Electronic structure

The theoretical calculation of the electronic structure by density functional theory (DFT) is very necessary to analyze the photoelectric properties of $CsPbI_3$ semiconductors. For $CsPbX_3$, its

valence band maximum (VBM) is mainly composed of antibonding hybridized Pb 6s and X np (dominant) orbitals, and the conduction band minimum (CBM) mainly consists of antibonding mixing of Pb 6p (dominant) and X np orbitals, as shown in Fig. 1c.[49] In addition, compared to $CsPbBr_3$ and $CsPbCl_3$, due to the large iodine radius, the geometric structure and electronic structure of $CsPbI_3$ change significantly, especially with respect to the band gap.[50] For example, the band gaps of the four different phases are cubic (α): 1.73 eV, tetragonal (β): 1.68 eV, orthorhombic (γ): 1.75 eV, and non-perovskite yellow phase (δ): 2.82 eV.[51]

3. The causes of $CsPbI_3$ instability

Generally, at RT, the black phase (α, β and γ) of the $CsPbI_3$ perovskite is metastable relative to the δ phase. Through analysis, we believe that the main reasons are as follows.

First, because the t of $CsPbI_3$ is too low (0.8472), it is close to the lowest limit of the perovskite structure, which is not conducive to phase stability.[47] Therefore, increasing the t can effectively improve the stability. Through the formula of t in Section 2.1, it can be found that increasing the radius of the A ion and reducing the radius of the B ion and X ion are effective measures.

Secondly, the Cs^+ has a very strong ionic bond with the $[PbX_6]^{4-}$ octahedron. This strong ionic bond can lead to crystal disorder and defect formation, so it is prone to cause phase transition and poor efficiency.

Third, $CsPbI_3$ is highly sensitive to polar solvents and moisture.[52] Once $CsPbI_3$ is exposed to a humid environment or encounters polar solvents, its black phase would convert to the yellow δ phase.[53] Tang *et al.* speculate that water molecules flow into the perovskite matrix and react to form intermediate hydrates, driving the phase transition.[54] Zhao *et al.* believe that the polar solvent tBP is not easy to volatilize and stay on the surface of the film due to its high boiling point, and that the nitrogen atoms on it and Pb^{2+} can form a strong coordination interaction, thereby inducing phase transition.[48] Therefore, stabilizing the $CsPbI_3$ perovskite is the top priority in the future.

4. Metastable phase based $CsPbI_3$ PSCs

Among all the black perovskite phases, though the α phase has a good band gap, it is usually obtained at high temperature (>320 °C). And the high temperature conditions are relatively harsh, which limits its development in other fields, such as flexible substrates. In addition, in a humid environment, it is easy to transform into the δ phase. Although many measures have been taken to improve stability and optimize performance, the current optimal PCE is based on the metastable phase.

Compared with the α phase, the β and γ phases can be realized at less than 200 °C or 100 °C.[51] The low-temperature preparation conditions expand its application in flexible solar cells, and its stability is relatively satisfying. Snaith *et al.* used the generalized gradient approximation (PBE) to calculate the formation energies of the four phases and analyze the reasons for better stability. They pointed out that due to the low formation energy of the γ phase, it is the most stable structure in the black phases, while the stability of the β phase is between that of the α phase and the γ phase, which is sub-stable.[55] Then, Huang *et al.* and Even *et al.* also used dissociation energy and density functional perturbation theory (DFPT), respectively, to conclude that the γ phase is the most stable phase in the black phase.[36,56] Huang *et al.* showed that the lower the dissociation energy is, the more stable the structure is. For the α, γ and δ phases, the dissociation energies are 0.04, −0.09 and −0.16 eV respectively, so the γ phase is more stable than the α phase. Even *et al.* calculated the phonon dispersion of the γ phase without any virtual mode at the Γ point, and no unstable phonons at other high symmetry points were found. And its total free energy was the lowest, further confirming the above statement. In addition, these phases can be analyzed and judged by X-ray diffraction (XRD). In XRD, relative to the single diffraction peak of the α phase, the metastable phase has split diffraction peaks, which indicates lower symmetry, as shown in Fig. 2a and b.[57,58]

In recent years, metastable phases have received extensive attention. Researchers have used different methods to improve performance and stability, and have made great progress. The photovoltaic parameters and preparation temperature are shown in Table 1. In this chapter, we will separately introduce the research and progress based on β and γ-$CsPbI_3$.

4.1 β-Phase

Compared with α-$CsPbI_3$, β-$CsPbI_3$ is formed by the deformation of the $[PbX_6]^{4-}$ octahedron, which can be prepared through various routes, as shown in Fig. 2c.[37] Among all black $CsPbI_3$ phases, β-$CsPbI_3$ does not have the best stability but it has a strong defect tolerance, which is conducive to obtaining higher performance. Recently, Chu *et al.* studied the non-radiative recombination process caused by native point defects in β-$CsPbI_3$.[59] They found that both shallow traps and deep traps are beneficial to inhibit charge recombination. And in the presence of defects, the soft inorganic lattice would deform, causing the separation of trapped charge and free charge, and allowing low-frequency motion to interact with electrons and holes. However, in experiments, there are still challenges in depositing stable β-$CsPbI_3$ PSCs, and research on the β phase is not much as well.

In 2017, Fu *et al.* prepared β-$CsPbI_3$ by using long-chain ammonium additives (phenylethylammonium (PEA)) at 120 °C, which acted as surface cap ligands to bind to the crystal surface, stabilize the perovskite structure, and further prevent grain growth and aggregation, as shown in Fig. 2d.[26] Finally, they obtained PSCs with a PCE of 6.5% and good phase stability at RT. Next, Zhao *et al.* spin-coated a precursor solution containing PbI_2·DMAI (dimethylammonium iodide) and CsI, and then prepared β-$CsPbI_3$ by annealing at 210 °C, and finally obtained a PCE of 15.1% with a significant hysteresis.[57] In order to

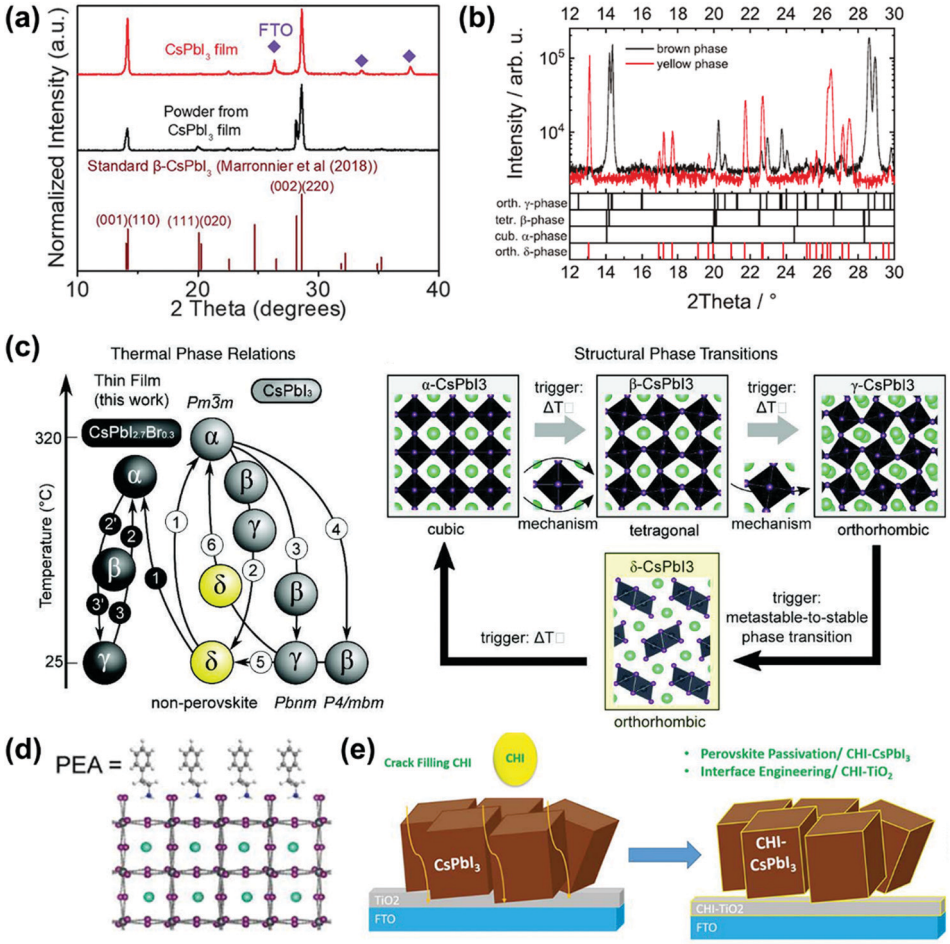

Fig. 2 (a) The XRD pattern of the $CsPbI_3$ film and the powder scraped from the film, the brown line is the XRD of β-$CsPbI_3$ determined by Marronnier *et al.* Reproduced with permission.[57] Copyright 2019, Science Publishing Group. (b) The XRD pattern of the brown and yellow areas of the sample. Reproduced with permission.[58] Copyright 2019, Wiley-VCH Publications. (c) Thermal phase relationship of $CsPbI_3$ (left), crystal structure and phase transition of different phases (right). Reproduced with permission.[37] Copyright 2019, Science Publishing Group. (d) Schematic diagram of the PEA stabilized γ-$CsPbI_3$ perovskite. Reproduced with permission.[26] Copyright 2017, American Chemical Society Publications. (e) Schematic diagram of the crack-filled interface. Reproduced with permission.[57] Copyright 2019, Science Publishing Group.

improve the PCE, they proposed a crack interface engineering method of using choline iodide (CHI), as shown in Fig. 2e. Unlike the conventional interface engineering that only passivates the upper surface of the perovskite, the crack interface engineering can not only treat the upper surface of β-$CsPbI_3$, but can also fill the holes and defects in the initial β-$CsPbI_3$ film. Through these microchannels, CHI is uniformly distributed on the upper and lower layers and inside of β-$CsPbI_3$, which can realize all-round modification of the perovskite. This omnidirectionally distributed CHI not only fully passivates the defects of the β-$CsPbI_3$ layer, but also optimizes the energy level matching between β-$CsPbI_3$ and the charge transport layer, thereby greatly improving the photovoltaic performance of the device. Finally, the β-$CsPbI_3$ PSCs based on defect repair and energy level optimization achieved a PCE of 18.4%. In the same year, they also used the same method to prepare β-$CsPbI_3$, and obtained the current best PCE of 19.03%.[60] Due to the different content of DMAI, γ-$CsPbI_3$ can also be produced, and we will focus on its mechanism in the next chapter.

4.2 γ-Phase

γ-$CsPbI_3$ can be prepared in two ways. One is to prepare α-$CsPbI_3$ at high temperature, and then rapidly cool in dry air to form the γ-phase, as shown in Fig. 3a. The other is to prepare the black phase at a temperature below 423 K by adding additives, usually hydride acid (HI). Compared with β-$CsPbI_3$, the Pb–I octahedron of γ-$CsPbI_3$ shows a higher degree of distortion, but it is the most stable structure in the black phases according to the above analysis, as shown in Fig. 3b.[55]

In general, the current research mainly bases on the following five aspects to improve the stability of γ-$CsPbI_3$:

(i) HI and its derivatives;
(ii) optimizing the tolerance factor;
(iii) improving the utilization of the solar spectrum;
(iv) low-dimensional perovskite;
(v) optimizing the preparation methods.

4.2.1 HI and its derivatives. HI is added as an additive to the perovskite precursor solution and has been extensively

Table 1 Summary of the progress of $CsPbI_3$ solar cells based on the metastable phase

Material	Methods	Configuration	Annealing temperature (°C)	*Jsc* [mA cm^{-2}]	*Voc* [V]	FF [%]	PCE [%]	Ref.
γ-$CsPbI_3$	HI and its derivatives	FTO/TiO_2/$CsPbI_3$/P3HT/Au	100	16.53	1.040	65.70	11.30	64
		FTO/TiO_2/$CsPbI_3$/PTAAAu	150	18.95	1.059	75.10	15.07	65
		FTO/PEDOT:PSS/$Cs_{0.7}DMA_{0.3}PbI_3$/C_{60}/BCP/Ag	100	16.65	0.990	76.49	12.62	63
	Optimizing the tolerance factor	FTO/TiO_2/$CsPb_{0.75}Ca_{0.25}I_3$/Spiro/Au	60	16.37	0.840	66.91	9.20	70
		FTO/TiO_2/$CsPbI_{2.85}Br_{0.15}$/PTAA/Au	—	19.75	1.135	76.60	17.17	71
		FTO/TiO_2/$CsPbI_3$:$Cl_{0.03}$/PTAA/Au	150	19.58	1.084	75.70	16.07	72
	Solar spectrum	N-CQDs EDS/FTO/TiO_2/$CsPbI_3$/PTAA/Au	150	19.15	1.106	75.60	16.02	24
		FTO/TiO_2/$CsPbI_3$/UCNP-doped PTAA/Au	150	19.17	1.113	74.33	15.86	75
	Low-dimensional perovskite	FTO/TiO_2/$(PEA)_2Cs_{n-1}Pb_nI_{3n+1}$/PTAA/Au	180	19.51	0.993	70.46	13.65	82
		FTO/TiO_2/$CsPbI_3$·0.5%$PZDI_2$/carbon	200	15.76	0.910	66.00	9.39	83
		ITO/PTAA/$CsPbI_3$ QNC/C_{60}/BCP/Cu	100	17.10	1.120	70.01	13.40	85
	Optimization of preparation methods	FTO/NiO_x/STCG-$CsPbI_3$/ZnO/ITO	100/150/200/250/300/350	18.29	1.090	80.50	16.04	86
		FTO/c-TiO_2/$CsPbI_3$/P3HT/Au	100/330	17.40	1.020	79.40	14.10	87
		ITO/PTAA/$CsPbI_3$/C_{60}/BCP/Cu	60	17.80	0.960	73.00	12.50	58
β-$CsPbI_3$	Additives	ITO/PEDOT:PSS/$CsPbI_3$/PCBM/Al	120	15.00	1.060	41.00	6.50	26
		FTO/c-TiO_2/$CsPbI_3$/Spiro/Ag	210	20.23	1.110	82.00	18.40	57
		FTO/TiO_2/$CsPbI_3$/Spiro/Ag	210	20.23	1.137	82.70	19.03	60

studied. Its effects are summarized as follows: (i) improving the solubility of the precursor material; (ii) reducing the phase transition temperature by inducing strain; (iii) forming small crystals and inducing high microstrain in the lattice to stabilize the $CsPbI_3$ perovskite;[53] (iv) high concentration of HI can adjust the content of iodide (I) and fill the I vacancies.[61] In addition, HI can also react with PbI_2 in DMF solution to generate intermediate $HPbI_3$. It avoids the water in the HI solution and can effectively improve the crystallinity of the perovskite.[62] Later someone said that because DMF hydrolyzes in HI solution, it is actually a compound of $DMAPbI_3$.[63] In addition, if only HI reacted with pure DMF, the result would be DMAI. Recently, Bian *et al.* used XRD, thermogravimetric analysis (TGA) and Fourier transform infrared reflectance (FTIR) spectra to explore in detail the HI hydrolysis derivative intermediate composed of $DMAI/DMAPbI_x$.[4] This intermediate compound can not only optimize the quality of the perovskite film, but also improve the humidity and thermal stability. And the $CsPbI_3$ film prepared after annealing is inorganic, with only a small amount of DMA^+ interacting with Pb^{2+} on the surface of the film, which has a passivation effect and reduces the recombination rate. The final PCE increased to 17.3%. In general, HI and its derivatives have been extensively studied due to their excellent properties in improving the performance of $CsPbI_3$.

For HI additives, in 2018, Zhao *et al.* prepared a stable γ-$CsPbI_3$ film by adding a small amount of H_2O to the $CsPbI_3$ precursor solution containing HI, in which the water molecules changed the size of the perovskite crystal through the proton transfer reaction, obtaining a PCE of 11.3%, as shown in Fig. 3c.[64] And through DFT calculations, it is found that γ-$CsPbI_3$ has a lower surface free energy than δ-$CsPbI_3$, so the thermodynamic stability has been improved, with no obvious loss in the performance of the device under an ambient environment for several months.

For its derivatives, in 2018, Wang *et al.* added HI and phenylethylammonium iodide (PEAI) additives to the precursor solution to prepare stable black γ-$CsPbI_3$ PSCs.[65] Here, HI induced the formation of the $HPbI_{3+x}$ intermediate, and PEAI optimized crystallization and blocked the phase transition through steric effects, as shown in Fig. 3d. Finally, a PCE of 15.07% was obtained, with the stability being improved. After being stored at RT for 2 months it still maintained 92% of its PCE. In the same year, Ke *et al.* reported that since $DMAPbI_3$ has a larger *t* (1.026), the *t* of the compound ($Cs_{1-x}DMA_xPbI_3$) could be adjusted by mixing DMA^+ and Cs^+ to reach the ideal value, as shown in Fig. 4a.[63] They also pointed out that this is an organic–inorganic hybrid perovskite and showed that the introduction of quantitative DMA^+ cations can achieve better performance than adding HI to the perovskite solution. This is mainly due to the addition of HI to the perovskite precursor, which makes it difficult to control the amount of DMA in the final film, and the performance improvement is mainly attributed to the better morphology and the incorporation of DMA^+ cations. Finally, the PSCs based on $Cs_{0.7}DMA_{0.3}PbI_3$ achieved a PCE of 12.62%. Next, Zhao *et al.* spin-coated a precursor solution containing CsI, PbI_2, and *x*DMAI (x = 0.5, 0.7, 1.0, 1.5) to prepare $CsPbI_3$. As a result, when x = 0.5, 0.7, γ-$CsPbI_3$ was formed, and when x = 1.0, 1.5, β-$CsPbI_3$ was formed. Through time-of-flight secondary ion mass spectrometry and nuclear magnetic resonance, it was proved that the DMAI additive did not participate in the $CsPbI_3$ lattice, which was of all inorganic composition.[60] DMAI was used as a volatile additive to control the crystallization process of different crystal phases and morphologies of the $CsPbI_3$ film, as shown in Fig. 4b. In addition, under an optimal amount of DMAI (x = 1.5), phenyltrimethylammonium chloride (PTACl) was added as a passivation agent. First, the organic cationic PTA^+ containing hydrophobic phenyl groups can improve the humidity stability and passivate surface defects. Secondly, since I defects appear on the surface of the film, and the chemical properties of chlorine (Cl) are very stable, it is difficult to oxidize it, so Cl can improve

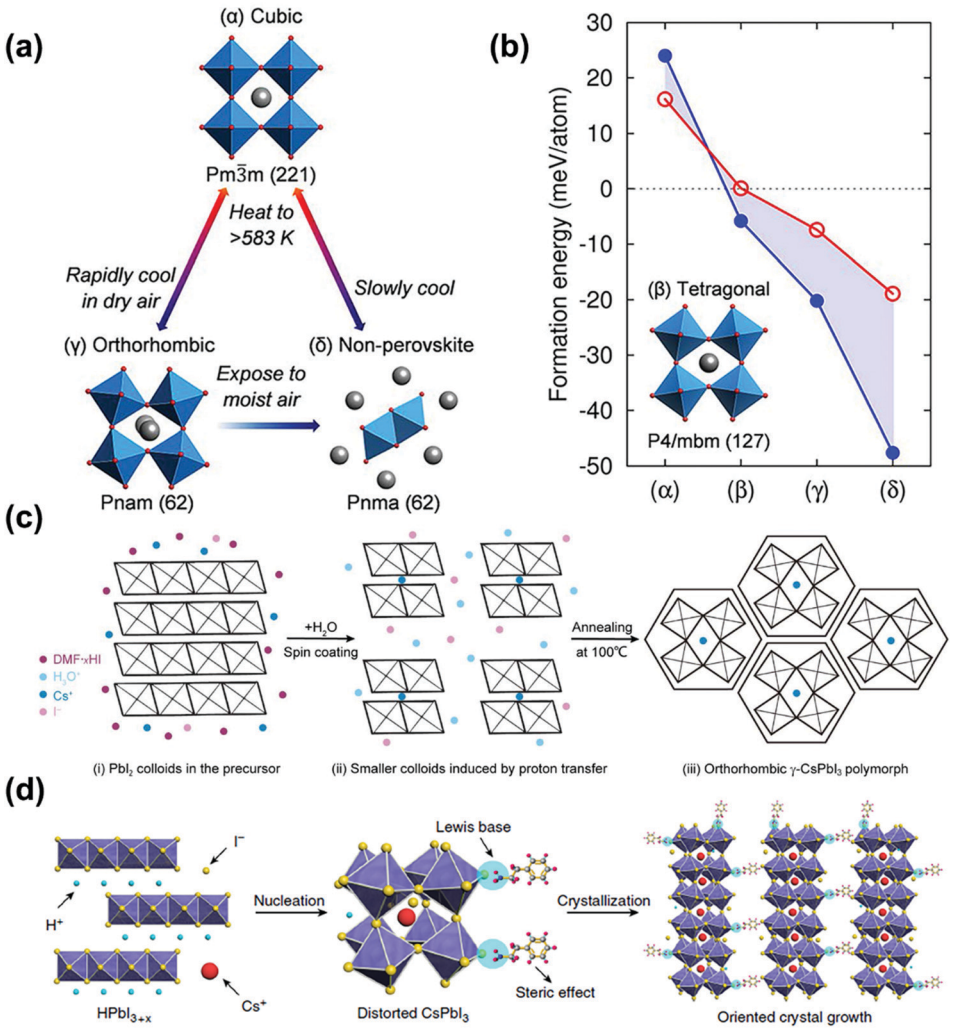

Fig. 3 (a) Models of different crystal phases and structural transformations of $CsPbI_3$. (b) The formation energy of different crystal phases of $CsPbI_3$. The red circles and lines are calculated by DFT/PBE calculations, and the blue dots and lines are calculated by DFT/LDA calculations. Reproduced with permission.[55] Copyright 2018, American Chemical Society Publications. (c) Method for preparing stable γ-$CsPbI_3$. (i) PbI_2 colloid is formed in the precursor solution. (ii) The addition of H_2O molecules promotes the release of H^+ and I^- from the DMF·xHI complex by HI, thereby forming a corner shared $[PbI_6]^{4-}$ octahedron intercalated by Cs^+ ions. (iii) The γ-$CsPbI_3$ with a small grain size is formed by thermal annealing. Reproduced with permission.[64] Copyright 2018, American Chemical Society Publications. (d) Schematic diagram of $CsPbI_3$ induced by HI/PEAI additives. Reproduced with permission.[65] Copyright 2018, Nature Publishing Group.

the stability by replacing I on the surface of the film. As a result, a device with good stability was obtained. After 500 hours of continuous light, 90% of the initial PCE was still retained.

4.2.2 Optimizing the tolerance factor. Since the *t* of $CsPbI_3$ is small, in addition to the $DMAPbI_3$ hybridization method mentioned above, *t* can also be optimized by the A-position, B-position, and X-position doping to improve the stability from its source. In $CsPbI_3$, Cs^+ is the largest one of the inorganic monovalent positive ions. The optimization of it is challenging with few research studies on this. The research is mainly about replacing Pb with some transition metals (such as Sn, Bi, Sr, Ge).[66,67] For example, Zhang *et al.* used Bi^{2+} to partially replace Pb^{2+} to distort the crystal lattice and generate micro-strain in the crystal lattice, thereby improving stability.[29] In addition, though X-site substitution increases the band gap, *t* can be optimized and different X-site elements can also increase carrier mobility and inhibit non-radiative recombination.[68,69] Next, we will focus on the research of B-site and X-site doping.

For the B-site doping, Zhao *et al.* used calcium ions (Ca^{2+}) with a small ion radius (100 pm) to partially replace Pb^{2+} (ion radius = 119 pm) to prepare stable γ-$CsPbI_3$ PSCs, as shown in Fig. 4c and d.[70] As a result, since Ca^{2+} was incorporated into γ-$CsPbI_3$, it resulted in a lower cohesive energy and a more suitable *t*. Therefore, the γ-$CsPbI_3$ formed at 60 °C was more stable than α-$CsPbI_3$ formed at >320 °C. Moreover, Ca^{2+} doping improved the morphology of the film and inhibited the recombination of carriers, and finally a PCE of 9.20% without hysteresis was obtained.

For the X-site doping, in 2019, Wang *et al.* achieved a record PCE of 17.17% by adding a small amount of Br^- to

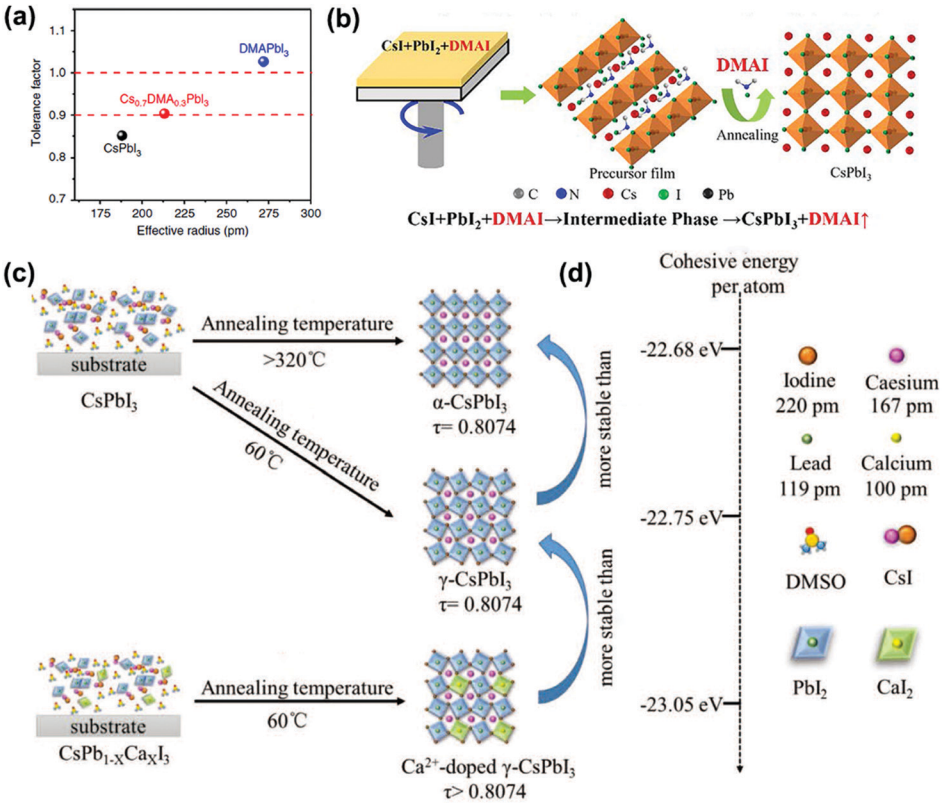

Fig. 4 (a) Tolerance factor of $CsPbI_3$, $DMAPbI_3$ and $Cs_{0.7}DMA_{0.3}PbI_3$. Reproduced with permission.[63] Copyright 2019, Nature Publishing Group. (b) Schematic diagram of the formation of black phase $CsPbI_3$ induced by DMAI. Reproduced with permission.[60] Copyright 2019, Wiley-VCH Publications. (c) Schematic diagram of the formation of α-$CsPbI_3$, γ-$CsPbI_3$ and Ca^{2+} doped γ-$CsPbI_3$. (d) Comparison of the cohesive energies of different phases calculated by the super soft pseudopotential method. Reproduced with permission.[70] Copyright 2019, Wiley-VCH Publications.

the $CsPbI_3$ film.[71] In this process, the addition of Br^- not only accelerated the entire crystallization process, helping to form a highly crystalline and uniform perovskite layer, but also improved the phase stability by effectively suppressing bulk trap-assisted nonradiative recombination and lattice strain relaxation. In the same year, they also added 3 mol% Cl^- to the γ-$CsPbI_3$ film and obtained a PCE of 16.07%. The incorporation of Cl^- can optimize the crystallization kinetics to obtain films with good surface morphology and crystal orientation.[72] In addition, it can also passivate the bulk and surface trap states to minimize the trap density and enhance the stability of the black phase. After being stored in an environment of RH ~ 30% for 60 days, it still maintained 94% of its initial PCE.

4.2.3 Improving the utilization of the solar spectrum. The solar spectrum ranges from 300 to 2500 nm, starting from ultraviolet (UV) to infrared (IR), but $CsPbI_3$ can only use visible light, and its utilization rate is relatively low, accounting for 49% of sunlight energy.[73–75] Reasonable development of UV light and IR light, converting them into useful visible photons, and further increasing the photocurrent are feasible ways to improve the performance of PSCs. Especially for $CsPbI_3$, its band gap (<1.73 eV) is not the most ideal value. Recent studies have focused on reducing the band gap to increase the collection rate of sunlight, and the energy-down-shift (EDS) layer can convert harmful ultraviolet rays into visible light.

In 2019, Jin *et al.* deposited nitrogen-doped graphene quantum dots (N-GQDs) on top of γ-$CsPbI_3$ PSCs, as shown in Fig. 5a.[24] As a result, N-GQDs with a photoluminescence quantum yield of 80% could form an EDS layer and converted ultraviolet light (<350 nm) that is harmful to the perovskite into useful visible light photons. At the same time, the short-circuit current density (J_{SC}) increased from 18.67 mA cm^{-2} to 19.15 mA cm^{-2}, and the PCE increased from 15.53% to 16.02%. Next, they introduced the core–shell structure $NaLuF_4$:Yb,Er@$NaLuF_4$ upconversion nanoparticles (UCNPs) into the hole transport layer, and obtained γ-$CsPbI_3$ PSCs with a J_{SC} of 19.17 mA cm^{-2} and a PCE of 15.8%.[75] As a result, they found that the upconversion effect of UCNPs was very small, mainly because UCNPs enhanced light scattering and reflection, increased the optical path length and reabsorption of the perovskite layer, which led to reabsorption of visible light and more photoelectric current, and also reduced the loss of solar energy.

4.2.4 Low-dimensional perovskite. Reducing the dimensionality and developing low-dimensional perovskites is another way to improve the stability of $CsPbI_3$. The restriction of structural instability caused by small t is applicable to 3D perovskites, but useless for low-dimensional PSCs (no restriction on the ionic radius of positions A, B and X).

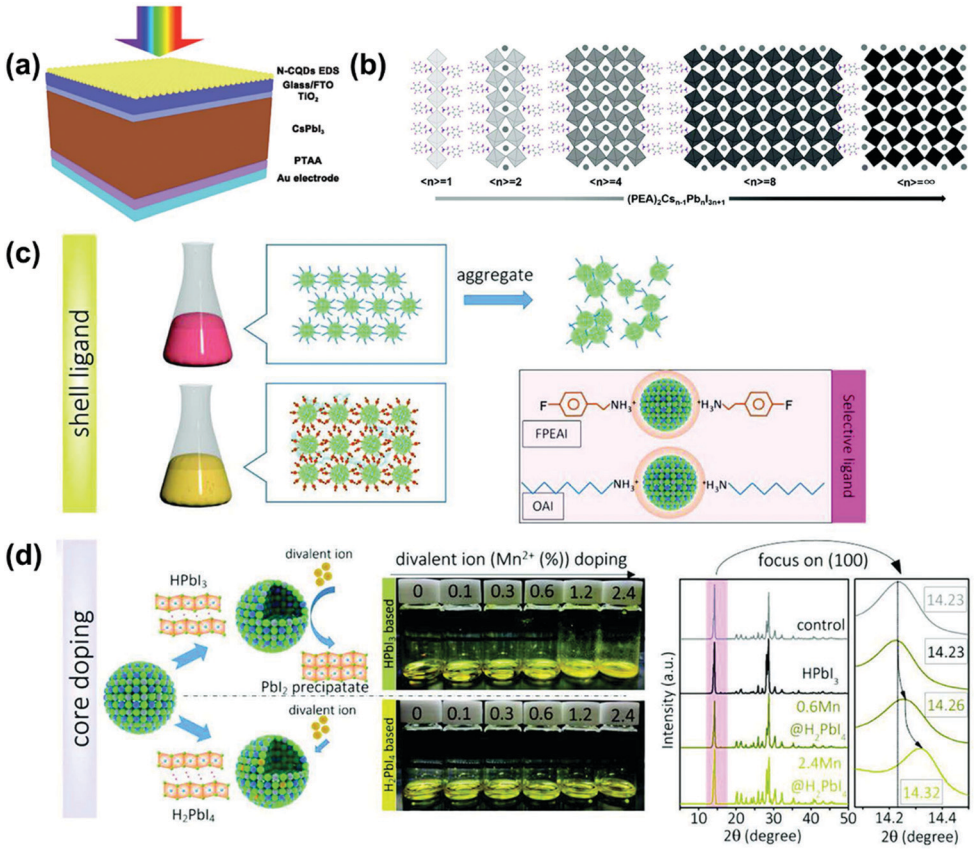

Fig. 5 (a) Schematic diagram of PSCs coated with N-GQDs. Reproduced with permission.[24] Copyright 2019, The Royal Society of Chemistry. (b) Schematic diagram of γ-$CsPbI_3$ in various dimensions. Reproduced with permission.[82] Copyright 2019, Wiley-VCH Publications. (c) Bonding interaction between nanocrystals limited by OAI and FPEAI ligands. (d) Based on $HPbI_3$ and excessive addition of H_2PbI_4 divalent ion (Mn^{2+}) doping process; the inset shows the XRD patterns of samples based on $HPbI_3$, 0.6% and 2.4% Mn^{2+} doped samples and the same amount of H_2PbI_4. Reproduced with permission.[85] Copyright 2019, Wiley-VCH Publications.

Low-dimensional perovskites mainly include the following: (i) 2D and quasi-2D structure: the layered structure composed of long hydrophobic cationic chains can not only be used as barrier molecules to prevent water erosion, component decomposition, phase change and oxidation, but also inhibit ion migration, thereby improving stability.[76,77] (ii): 2D/3D mixed-phase: combining the stability of 2D perovskites with the excellent charge transport characteristics of 3D perovskites to prepare efficient and stable $CsPbI_3$.[78] (iii) 0D quantum dots (QDs)/nanocrystals (NCs): reducing the crystal size can lead to more surface accommodation of organic groups, which can cause surface strain. At the same time, due to the strong quantum confinement effect and the high surface Gibbs energy contributed by the large surface/volume ratio, $CsPbI_3$ QDs themselves are thermodynamically stable. And the most suitable α-phase for its band gap is very stable, and it is worthy of further investigation.[79–81] In this part, we will focus on the progress of $CsPbI_3$ based on 2D and QD structure.

In 2019, Wang *et al.* introduced the 2D Ruddlesden–Popper $(PEA)_2(Cs)_{n-1}Pb_n I_{3n+1}$ structure in γ-$CsPbI_3$.[82] Adding different amounts of PEAI to the $DMAPbI_3$ precursor solution can adjust the size of the γ-$CsPbI_3$ film from a 2D structure to a quasi 2D and 3D structure, as shown in Fig. 5b. As a result, as the content of PEAI increased, crystal orientation, film morphology and water resistance were improved. Moreover, the film with $n = 40$ exhibited charge extraction and carrier lifetime similar to that of 3D samples, and its stability was greatly improved with the best PCE of 13.65%. Then, Chen *et al.* first used a new type of piperazine-1,4-diium iodide ($PZDI_2$) as the intermediate layer, which was inserted between the layered perovskites to form 2D RP $CsPbI_3$.[83] Finally, the device achieved a PCE of 9.39% without any degradation in performance after being placed at RT for 1200 h.

In addition to 2D PSCs, for the self-stable QDs, we will briefly introduce the progress of how they form films to help readers further develop $CsPbI_3$ QD PSCs. In 2018, Pradhan *et al.* prepared stable $CsPbI_3$ NCs at a high temperature (260 °C) by adding appropriate amounts of oleylamine (OLA) and hydroiodic acid (HI) to the reaction system.[84] And through NMR analysis, it was revealed that under high temperature conditions, the introduced OLA^+ replaced Cs^+ to firmly passivate the surface and prevent the phase change of the NCs. Although stable $CsPbI_3$ NCs have been successfully prepared, it was difficult to assemble these NCs into thin films. The essential problem was the unfavorable shell ligands and unstable core lattices in the NCs. In order to solve this problem, Choi *et al.*

proposed a reasonable core–shell design.[85] They first adopted a new 4-fluorophenylammonium iodide (FPEAI) to enhance the bonding force and charge coupling between the ligand and the NCs, as shown in Fig. 5c. In addition, they used the new compound H_2PbI_4 to assist the doping of divalent ions (Mn^{2+}) into the perovskite lattice, as shown in Fig. 5d. Mn^{2+} was used as a doping agent because its higher formation energy can prevent the formation of other non-perovskites. As a result, they prepared $CsPbI_3$ PSCs with the highest PCE of 13.4%, and their stability had been greatly improved. After the unpackaged device was exposed to ambient air for 500 h, it still maintained 92% of its original PCE.

4.2.5 Optimizing preparation methods. In addition to the conventional solution method mentioned above, the optimization of the preparation method can also further improve the stability of $CsPbI_3$. In 2020, Cheng *et al.* proposed a simple soft template controlled growth (STCG) method.[86] They used (Adamantan-1-yl) methylammonium (ADMA) as a soft template, adsorbed this on the surface of the $CsPbI_3$ crystal, and increased the nucleation rate as much as possible at the beginning, and then adjusted the growth rate by adjusting the annealing temperature, as shown in Fig. 6a. As a result, a pinhole-free and high-quality γ-$CsPbI_3$ film with a PCE of 16.04% was obtained.

Then Lau *et al.* also proposed a simple cation exchange growth (CEG) method to prepare γ-$CsPbI_3$.[87] Specifically, they first prepared the $MAPbI_3$ perovskite template, and then replaced the organic MA^+ with Cs^+ at high temperature to form a dense film without pinholes. Finally, they obtained a PCE of 14.1%, which is much higher than that obtained by the traditional method (8.9%), as shown in Fig. 6b.

In addition to the above two methods, Becker *et al.* also proposed to prepare γ-$CsPbI_3$ by co-evaporating CsI and PbI_2 at

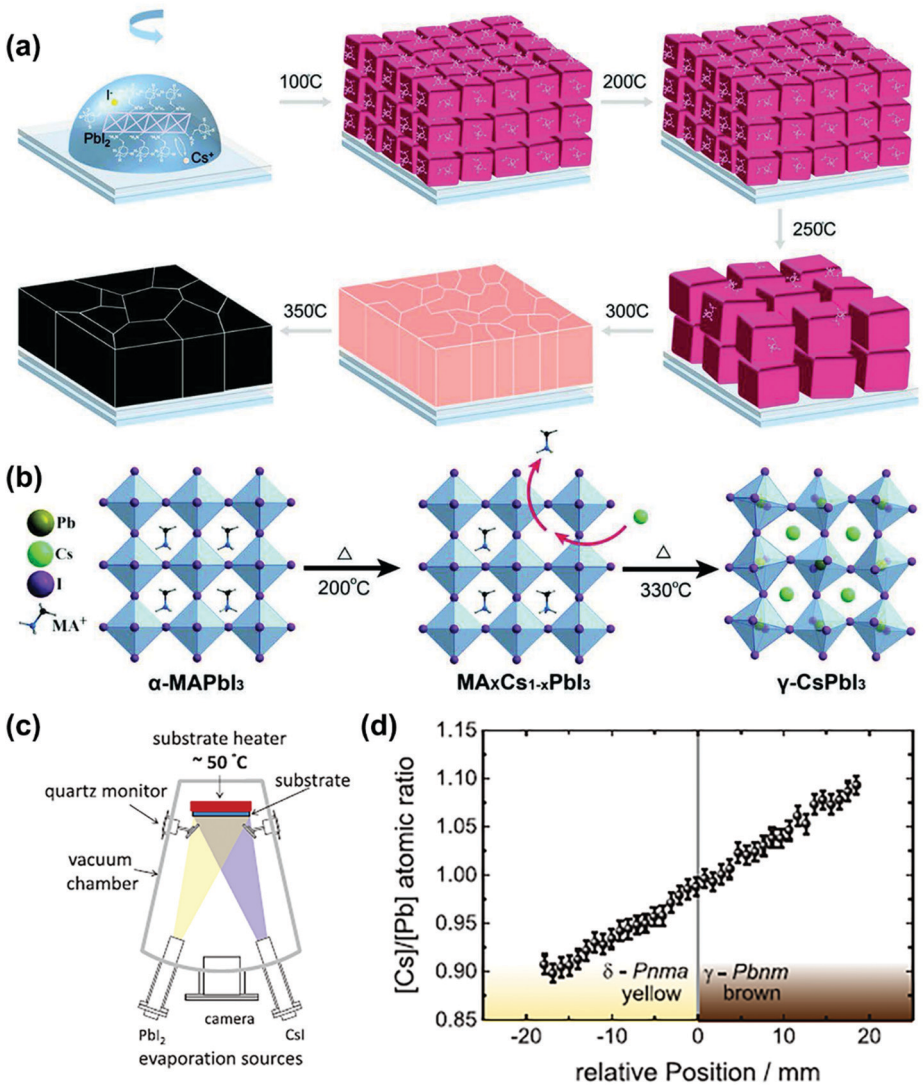

Fig. 6 (a) Preparation of $CsPbI_3$ films using the STCG method. Reproduced with permission.[86] Copyright 2020, Wiley-VCH Publications. (b) Preparation of $CsPbI_3$ crystals using the cation exchange growth method. Reproduced with permission.[87] Copyright 2019, Wiley-VCH Publications. (c) Schematic diagram of co-evaporation deposited film. (d) The relationship between the atomic ratio of [Cs]/[Pb] and the position perpendicular to the phase boundary. Reproduced with permission.[58] Copyright 2019, Wiley-VCH Publications.

a substrate temperature of 50 °C without post-deposition annealing treatment, as shown in Fig. 6c.[58] They found that under CsI-rich conditions, γ-$CsPbI_3$ can be directly prepared, while PbI-rich conditions are beneficial to the formation of a non-perovskite, as shown in Fig. 6d. As a result, a device with efficiency exceeding 12% and stability (over 1200 hours) was obtained.

5. Challenges and outlook

In summary, though $CsPbI_3$ PSCs based on metastable phases have achieved a PCE of beyond 19% which is a great progress, their efficiency still lags behind that of PSCs based on organic–inorganic hybrid perovskites, and their stability is unsatisfactory for commercial requirements. Therefore, in this section, we summarize the current problems and challenges faced by $CsPbI_3$ PSCs, and put forward our own suggestions and prospects.

5.1 Challenges

• Although many measures have been taken to optimize the performance and improve stability, $CsPbI_3$ still undergoes a phase change when it encounters a polar solvent and its stability is not good enough as well. In particular, water molecules in the air also accelerate the collapse of the perovskite structure, leading to a phase change. This thermodynamic instability hinders its practical application and is currently the biggest challenge that needs to be solved urgently.

• The best PCE of $CsPbI_3$ is only 70% of the efficiency limit of Shockley–Queisser (S–Q), and its open circuit voltage (V_{OC}) is 1.137 V, which is about 0.5 V loss from the ideal value.[34,60] This may be due to energy level mismatch, high defect density and short carrier lifetime, which also limit the further improvement of efficiency.

• The way of judging the metastable phase is not clear. Recently, studies have shown that the previous α phase is actually the γ phase.[88,89] But there is no good explanation for this phenomenon. At present, most judgments rely on XRD. For β-phase and γ-phase, it can be judged from the size of the essential Pb–I–Pb bond angle. Therefore, it is challenging to explore more identification methods to distinguish the metastable phase.

• The scalable fabrication of $CsPbI_3$ PSCs faces many challenges such as low PCE, poor long-term stability, and high production costs.[90] Specifically, compared with organic–inorganic hybrid PSCs, although the thermal stability of $CsPbI_3$ PSCs is better, their PCE is lower. In addition, they are prone to phase change, which requires better packaging technology for industrial development, which will increase the cost.

5.2 Future outlooks

At present, the research on metastable phases has been widely carried out, but there are still many valuable issues worthy of discussion. The following are the directions that we think are worth studying in the future.

• The essence of $CsPbI_3$ is thermodynamically unstable, so we can improve the stability by the following methods. For example, the introduction of steric hindrance inhibits the inclination of the $[PbX_6]^{4-}$ octahedron and then prevents its transformation into the δ phase. In addition, reducing the crystal size and developing low-dimensional perovskites can also improve stability. Current research mostly bases on 3D perovskites.[52] There are few studies on QDs, 2D β-$CsPbI_3$ and γ-$CsPbI_3$. Compared with 3D perovskites, they have better stability, but due to the introduction of long molecular chains, they have low carrier transport and a limited PCE.[91,92] Therefore, in the future, low-dimensional perovskites could be developed with increasing carrier transport to prepare stable and efficient $CsPbI_3$ PSCs.

• Optimizing crystallization to improve chemical stability. The quality of the $CsPbI_3$ film plays an important role in optimizing the performance of the device. There are a large number of defects on the surface and inside of $CsPbI_3$, which can be used as charge recombination centers, reducing the carrier lifetime and causing energy loss.[93] Therefore, the preparation of a dense, pinhole-free $CsPbI_3$ film with fewer defects and exploring new additives for grain boundary passivation are good ways to improve stability in the future.

• Developing stable charge transport materials and electrode materials. The easy phase transition of the $CsPbI_3$ perovskite is partly due to the promotion of moisture in the air. If a stable pure inorganic transport layer and a low-cost moisture-proof carbon electrode are developed on the upper layer of the perovskite, these not only optimize charge extraction and the energy level position, but also play the role of encapsulation to prevent moisture from entering and improve stability.[94–96]

• The current standards for determining β-phase and γ-phase are too few. In the future, other methods, such as *in situ* electron microscopy, can be combined with cooling conditions to observe, in real time, the degree of distortion of each phase during the phase transition. Establishing a criterion for the judgment of metastable state is worthy of more exploration.

• Most of the current scalable fabrication methods are based on organic–inorganic hybrid PSCs. There is little research on Cs-based PSCs, and there is a lot of room for development. The precursor solution, preparation method, and component design suitable for large area Cs-based PSCs are worthy of research and exploration.[97]

In general, a lot of efforts have been made to improve the performance and stability of $CsPbI_3$, but there remains a lot of room for the S–Q limit, which is worth exploring.[98] Besides, the suitable band gap (1.73 eV) of $CsPbI_3$ makes it suitable for the top cell of perovskite/silicon tandem solar cells.[99] But the high band gap $CsPbI_3$ PSCs have a large V_{OC} loss, and the lowest value is 0.41 V, resulting in a poor efficiency.[100] In addition, the phase stability is poor, and it is easy to become δ phase under environmental conditions, so the current research is still in its infancy and it is worth exploring. In any case, we should treat $CsPbI_3$ PSCs with an optimistic attitude and propose better methods to solve the current problems.

Conflicts of interest

The authors declare no competing financial interests.

Acknowledgements

This work was funded by the National Natural Science Foundation of China (52073131, 51902148, 61704099, 61874166, U1832149, 51801088 and 51802024), the Natural Science Foundation of Gansu Province (20JR5RA227, 20JR5RA217 and 20JR5RA278), and the Fundamental Research Funds for the Central Universities (lzujbky-2020-61, lzujbky-2019-88 and lzujbky-2020-kb06).

References

1 A. Kojima, K. Teshima, Y. Shirai and T. Miyasaka, Organometal Halide Perovskites as Visible-Light Sensitizers for Photovoltaic Cells, *J. Am. Chem. Soc.*, 2009, **131**, 6050–6051.
2 NREL, https://www.nrel.gov/pv/device-performance.html (accessed:October 2020). 2020.
3 J. Zhang, G. Hodes, Z. Jin and S. Liu, All-Inorganic $CsPbX_3$ Perovskite Solar Cells: Progress and Prospects, *Angew. Chem., Int. Ed.*, 2019, **58**, 15596–15618.
4 H. Bian, H. Wang, Z. Li, F. Zhou, Y. Xu, H. Zhang, Q. Wang, L. Ding, S. Liu and Z. Jin, Unveiling the Effects of Hydrolysis-Derived DMAI/$DMAPbI_x$ Intermediate Compound on Performance of $CsPbI_3$ Solar Cells, *Adv. Sci.*, 2020, **7**, 1902868.
5 L. Zhou, X. Guo, Z. Lin, J. Ma, J. Su, Z. Hu, C. Zhang, S. Liu, J. Chang and Y. Hao, Interface Engineering of Low Temperature Processed All-Inorganic $CsPbI_2Br$ Perovskite Solar Cells Toward PCE Exceeding 14%, *Nano Energy*, 2019, **60**, 583–590.
6 G. Liu, B. Yang, B. Liu, C. Zhang, S. Xiao, Y. Yuan, H. Xie, D. Niu, J. Yang, Y. Gao and C. Zhou, Irreversible Light-Soaking Effect of Perovskite Solar Cells Caused by Light-Induced Oxygen Vacancies in Titanium Oxide, *Appl. Phys. Lett.*, 2017, **111**, 3501.
7 B. Liu, M. Long, M.-Q. Cai and J. Yang, Influence of The Number of Layers on Ultrathin $CsSnI_3$ Perovskite: From Electronic Structure to Carrier Mobility, *J. Phys. D: Appl. Phys.*, 2018, **51**, 5101.
8 W. Hu, H. Cong, W. Huang, Y. Huang, L. Chen, A. Pan and C. Xue, Germanium/perovskite Heterostructure for High-Performance And Broadband Photodetector From Visible to Infrared Telecommunication Band, *Light: Sci. Appl.*, 2019, **8**, 106.
9 S. B. Kang, J.-H. Kim, M. H. Jeong, A. Sanger, C. U. Kim, C.-M. Kim and K. J. Choi, Stretchable And Colorless Freestanding Microwire Arrays for Transparent Solar Cells with Flexibility, *Light: Sci. Appl.*, 2019, **8**, 121.
10 K. O. Brinkmann, J. Zhao, N. Pourdavoud, T. Becker, T. Hu, S. Olthof, K. Meerholz, L. Hoffmann, T. Gahlmann, R. Heiderhoff, M. F. Oszajca, N. A. Luechinger, D. Rogalla, Y. Chen, B. Cheng and T. Riedl, Suppressed Decomposition of Organometal Halide Perovskites by Impermeable Electron-Extraction Layers in Inverted Solar Cells, *Nat. Commun.*, 2017, **8**, 13938.
11 J. Jiang, Q. Wang, Z. Jin, X. Zhang, J. Lei, H. Bin, Z.-G. Zhang, Y. Li and S. Liu, Polymer Doping for High-Efficiency Perovskite Solar Cells with Improved Moisture Stability, *Adv. Energy Mater.*, 2018, **8**, 1701757.
12 N. Chen, X. Yi, J. Zhuang, Y. Wei, Y. Zhang, F. Wang, S. Cao, C. Li and J. Wang, An Efficient Trap Passivator for Perovskite Solar Cells: Poly(propylene glycol) bis(2-aminopropyl ether), *Nano-Micro Lett.*, 2020, **12**, 177.
13 H.-H. Fang, F. Wang, S. Adjokatse, N. Zhao, J. Even and M. Antonietta Loi, Photoexcitation Dynamics in Solution-Processed Formamidinium Lead Iodide Perovskite Thin Films for Solar Cell Applications, *Light: Sci. Appl.*, 2016, **5**, e16056.
14 J. Xiong, B. Yang, C. Cao, R. Wu, Y. Huang, J. Sun, J. Zhang, C. Liu, S. Tao, Y. Gao and J. Yang, Interface Degradation of Perovskite Solar Cells And Its Modification Using An Annealing-Free TiO_2 NPs Layer, *Org. Electron.*, 2016, **30**, 30–35.
15 Y.-C. Zhao, W.-K. Zhou, X. Zhou, K.-H. Liu, D.-P. Yu and Q. Zhao, Quantification of Light-Enhanced Ionic Transport in Lead Iodide Perovskite Thin Films And Its Solar Cell Applications, *Light: Sci. Appl.*, 2017, **6**, e16243.
16 Y. Liu, C. Xie, W. Tan, X. Liu, Y. Yuan, Q. Xie, Y. Li and Y. Gao, Analysis of Light-Induced Degradation in Inverted Perovskite Solar Cells under Short-Circuited Conditions, *Org. Electron.*, 2019, **71**, 123–130.
17 J.-F. Wang, D.-X. Lin and Y.-B. Yuan, Recent Progress of Ion Migration in Organometal Halide Perovskite, *Acta Phys. Sin.*, 2019, **68**, 158801.
18 X. Jia, C. Zuo, S. Tao, K. Sun, Y. Zhao, S. Yang, M. Cheng, M. Wang, Y. Yuan, J. Yang, F. Gao, G. Xing, Z. Wei, L. Zhang, H.-L. Yip, M. Liu, Q. Shen, L. Yin, L. Han, S. Liu, L. Wang, J. Luo, H. Tan, Z. Jin and L. Ding, $CsPb(I_xBr_{1-x})_3$ Solar Cells, *Sci. Bull.*, 2019, **64**, 1532–1539.
19 T. Burwig, W. Fränzel and P. Pistor, Crystal Phases and Thermal Stability of Co-Evaporated $CsPbX_3$ (X = I, Br) Thin Films, *J. Phys. Chem. Lett.*, 2018, **9**, 4808–4813.
20 J. Ma, J. Su, Z. Lin, L. Zhou, J. He, J. Zhang, S. Liu, J. Chang and Y. Hao, Improve the Oxide/Perovskite Heterojunction Contact for Low Temperature High Efficiency and Stable All-Inorganic $CsPbI_2Br$ Perovskite Solar Cells, *Nano Energy*, 2020, **67**, 104241.
21 L. Zhou, J. Su, Z. Lin, X. Guo, J. Ma, L. Feng, J. Zhang, S. Wang, S. Liu, J. Chang and Y. Hao, Deep-Ultraviolet Photoactivation-Assisted Contact Engineering Toward High-Efficiency and Stable All-Inorganic $CsPbI_2Br$ Perovskite Solar Cells, *Sol. RRL*, 2020, **4**, 2070061.
22 J. Zhang, D. Bai, Z. Jin, H. Bian, K. Wang, J. Sun, Q. Wang and S. Liu, 3D-2D-0D Interface Profiling for Record Efficiency All-Inorganic $CsPbBrI_2$ Perovskite Solar Cells with Superior Stability, *Adv. Energy Mater.*, 2018, **8**, 1703246.
23 Y. Gao, Y. Dong, K. Huang, C. Zhang, B. Liu, S. Wang, J. Shi, H. Xie, H. Huang, S. Xiao, J. He, Y. Gao, R. A. Hatton

and J. Yang, Highly Efficient, Solution-Processed $CsPbI_2Br$ Planar Heterojunction Perovskite Solar Cells *via* Flash Annealing, *ACS Photonics*, 2018, **5**, 4104–4110.

24 H. Bian, Q. Wang, S. Yang, C. Yan, H. Wang, L. Liang, Z. Jin, G. Wang and S. Liu, Nitrogen-Doped Graphene Quantum Dots for 80% Photoluminescence Quantum Yield for Inorganic γ-$CsPbI_3$ Perovskite Solar Cells with Efficiency beyond 16%, *J. Mater. Chem. A*, 2019, **7**, 5740–5747.

25 Y. Zhou and Y. Zhao, Chemical Stability and Instability of Inorganic Halide Perovskites, *Energy Environ. Sci.*, 2019, **12**, 1495–1511.

26 Y. Fu, M. T. Rea, J. Chen, D. J. Morrow, M. P. Hautzinger, Y. Zhao, D. Pan, L. H. Manger, J. C. Wright, R. H. Goldsmith and S. Jin, Selective Stabilization and Photophysical Properties of Metastable Perovskite Polymorphs of $CsPbI_3$ in Thin Films, *Chem. Mater.*, 2017, **29**, 8385–8394.

27 J. Jiang, Z. Jin, F. Gao, J. Sun, Q. Wang and S. Liu, $CsPbCl_3$-Driven Low-Trap-Density Perovskite Grain Growth for >20% Solar Cell Efficiency, *Adv. Sci.*, 2018, **5**, 1800474.

28 L. Li, H. Chen, Z. Fang, X. Meng, C. Zuo, M. Lv, Y. Tian, Y. Fang, Z. Xiao, C. Shan, Z. Xiao, Z. Jin, G. Shen, L. Shen and L. Ding, An Electrically Modulated Single-Color/Dual-Color Imaging Photodetector, *Adv. Mater.*, 2020, **32**, 1907257.

29 Y. Hu, F. Bai, X. Liu, Q. Ji, X. Miao, T. Qiu and S. Zhang, Bismuth Incorporation Stabilized α-$CsPbI_3$ for Fully Inorganic Perovskite Solar Cells, *ACS Energy Lett.*, 2017, **2**, 2219–2227.

30 X. Zhang, Q. Wang, Z. Jin, J. Zhang and S. Liu, Stable Ultra-Fast Broad-Bandwidth Photodetectors Based on α-$CsPbI_3$ Perovskite and $NaYF_4$:Yb,Er Quantum Dots, *Nanoscale*, 2017, **9**, 6278–6285.

31 F. Zhou, Z. Li, H. Chen, Q. Wang, L. Ding and Z. Jin, Application of Perovskite Nanocrystals (NCs)/Quantum Dots (QDs) in Solar Cells, *Nano Energy*, 2020, **73**, 104757.

32 Z. Li, F. Zhou, Q. Wang, L. Ding and Z. Jin, Approaches for Thermodynamically Stabilized $CsPbI_3$ Solar Cells, *Nano Energy*, 2020, **71**, 104634.

33 N. A. N. Ouedraogo, Y. Chen, Y. Y. Xiao, Q. Meng, C. B. Han, H. Yan and Y. Zhang, Stability of All-Inorganic Perovskite Solar Cells, *Nano Energy*, 2020, **67**, 104249.

34 J. Tian, Q. Xue, Q. Yao, N. Li, C. J. Brabec and H.-L. Yip, Inorganic Halide Perovskite Solar Cells: Progress and Challenges, *Adv. Energy Mater.*, 2020, **10**, 2000183.

35 J. Klarbring, Low-Energy Paths for Octahedral Tilting in Inorganic Halide Perovskites, *Phys. Rev. B: Condens. Matter Mater. Phys.*, 2019, **99**, 104105.

36 A. Marronnier, G. Roma, S. Boyer-Richard, L. Pedesseau, J.-M. Jancu, Y. Bonnassieux, C. Katan, C. C. Stoumpos, M. G. Kanatzidis and J. Even, Anharmonicity and Disorder in the Black Phases of Cesium Lead Iodide Used for Stable Inorganic Perovskite Solar Cells, *ACS Nano*, 2018, **12**, 3477–3486.

37 J. A. Steele, H. Jin, I. Dovgaliuk, R. F. Berger, T. Braeckevelt, H. Yuan, C. Martin, E. Solano, K. Lejaeghere, S. M. J. Rogge, C. Notebaert, W. Vandezande, K. P. F. Janssen, B. Goderis, E. Debroye, Y.-K. Wang, Y. Dong, D. Ma, M. Saidaminov, H. Tan, Z. Lu, V. Dyadkin, D. Chernyshov, V. Van Speybroeck, E. H. Sargent, J. Hofkens and M. B. J. Roeffaers, Thermal Unequilibrium of Strained Black $CsPbI_3$ Thin Films, *Science*, 2019, **365**, 679–684.

38 M. A. Green, A. Ho-Baillie and H. J. Snaith, The Emergence of Perovskite Solar Cells, *Nat. Photonics*, 2014, **8**, 506–514.

39 Y. Zhao and K. Zhu, Organic–inorganic Hybrid Lead Halide Perovskites for Optoelectronic and Electronic Applications, *Chem. Soc. Rev.*, 2016, **45**, 655–689.

40 A. J. Ramadan, L. A. Rochford, S. Fearn and H. J. Snaith, Processing Solvent-Dependent Electronic and Structural Properties of Cesium Lead Triiodide Thin Films, *J. Phys. Chem. Lett.*, 2017, **8**, 4172–4176.

41 Z. Li, M. Yang, J.-S. Park, S.-H. Wei, J. J. Berry and K. Zhu, Stabilizing Perovskite Structures by Tuning Tolerance Factor: Formation of Formamidinium and Cesium Lead Iodide Solid-State Alloys, *Chem. Mater.*, 2016, **28**, 284–292.

42 G. Kieslich, S. Sun and A. K. Cheetham, Solid-state Principles Applied to Organic–inorganic Perovskites: New Tricks for an Old Dog, *Chem. Sci.*, 2014, **5**, 4712–4715.

43 S.-Q. Luo, J.-F. Wang, B. Yang and Y.-B. Yuan, Recent Advances in Controlling the Crystallization of Two-Dimensional Perovskites for Optoelectronic Device, *Front. Phys.*, 2019, **14**, 53401.

44 C. Ortiz-Cervantes, P. Carmona-Monroy and D. Solis-Ibarra, Two-Dimensional Halide Perovskites in Solar Cells: 2D or not 2D?, *ChemSusChem*, 2019, **12**, 1560–1575.

45 A. Dutta and N. Pradhan, Phase-Stable Red-Emitting $CsPbI_3$ Nanocrystals: Successes and Challenges, *ACS Energy Lett.*, 2019, **4**, 709–719.

46 I. Lignos, V. Morad, Y. Shynkarenko, C. Bernasconi, R. M. Maceiczyk, L. Protesescu, F. Bertolotti, S. Kumar, S. T. Ochsenbein, N. Masciocchi, A. Guagliardi, C.-J. Shih, M. I. Bodnarchuk, A. J. deMello and M. V. Kovalenko, Exploration of Near-Infrared-Emissive Colloidal Multinary Lead Halide Perovskite Nanocrystals Using an Automated Microfluidic Platform, *ACS Nano*, 2018, **12**, 5504–5517.

47 J.-K. Sun, S. Huang, X.-Z. Liu, Q. Xu, Q.-H. Zhang, W.-J. Jiang, D.-J. Xue, J.-C. Xu, J.-Y. Ma, J. Ding, Q.-Q. Ge, L. Gu, X.-H. Fang, H.-Z. Zhong, J.-S. Hu and L.-J. Wan, Polar Solvent Induced Lattice Distortion of Cubic $CsPbI_3$ Nanocubes and Hierarchical Self-Assembly into Orthorhombic Single-Crystalline Nanowires, *J. Am. Chem. Soc.*, 2018, **140**, 11705–11715.

48 J. Zhao, Y. Xu, H. Wang, Z. Li, H. Yao, W. Lan, Q. Wang and Z. Jin, Unveiling the Effects of Intrinsic and Extrinsic Factors That Induced a Phase Transition for $CsPbI_3$, *ACS Appl. Energy Mater.*, 2020, **3**, 8184–8189.

49 V. K. Ravi, G. B. Markad and A. Nag, Band Edge Energies and Excitonic Transition Probabilities of Colloidal $CsPbX_3$ (X = Cl, Br, I) Perovskite Nanocrystals, *ACS Energy Lett.*, 2016, **1**, 665–671.

50 X. Li, F. Cao, D. Yu, J. Chen, Z. Sun, Y. Shen, Y. Zhu, L. Wang, Y. Wei, Y. Wu and H. Zeng, All Inorganic Halide

Perovskites Nanosystem: Synthesis, Structural Features, Optical Properties and Optoelectronic Applications, *Small*, 2017, **13**, 1603996.

51 Q. Ye, Y. Zhao, S. Mu, P. Gao, X. Zhang and J. You, Stabilizing the Black Phase of Cesium Lead Halide Inorganic Perovskite for Efficient Solar Cells, *Sci. China: Chem.*, 2019, **62**, 810–821.

52 T. Wu, Y. Wang, Z. Dai, D. Cui, T. Wang, X. Meng, E. Bi, X. Yang and L. Han, Efficient and Stable $CsPbI_3$ Solar Cells *via* Regulating Lattice Distortion with Surface Organic Terminal Groups, *Adv. Mater.*, 2019, **31**, 1900605.

53 G. E. Eperon, G. M. Paternò, R. J. Sutton, A. Zampetti, A. A. Haghighirad, F. Cacialli and H. J. Snaith, Inorganic Caesium Lead Iodide Perovskite Solar Cells, *J. Mater. Chem. A*, 2015, **3**, 19688–19695.

54 W. Ahmad, J. Khan, G. Niu and J. Tang, Inorganic $CsPbI_3$ Perovskite-Based Solar Cells: A Choice for a Tandem Device, *Sol. RRL*, 2017, **1**, 1700048.

55 R. J. Sutton, M. R. Filip, A. A. Haghighirad, N. Sakai, B. Wenger, F. Giustino and H. J. Snaith, Cubic or Orthorhombic? Revealing the Crystal Structure of Metastable Black-Phase $CsPbI_3$ by Theory and Experiment, *ACS Energy Lett.*, 2018, **3**, 1787–1794.

56 Y. Huang, W.-J. Yin and Y. He, Intrinsic Point Defects in Inorganic Cesium Lead Iodide Perovskite $CsPbI_3$, *J. Phys. Chem. C*, 2018, **122**, 1345–1350.

57 Y. Wang, M. I. Dar, L. K. Ono, T. Zhang, M. Kan, Y. Li, L. Zhang, X. Wang, Y. Yang, X. Gao, Y. Qi, M. Grätzel and Y. Zhao, Thermodynamically Stabilized β-$CsPbI_3$–Based Perovskite Solar Cells with Efficiencies >18%, *Science*, 2019, **365**, 591–595.

58 P. Becker, J. A. Márquez, J. Just, A. Al-Ashouri, C. Hages, H. Hempel, M. Jošt, S. Albrecht, R. Frahm and T. Unold, Low Temperature Synthesis of Stable γ-$CsPbI_3$ Perovskite Layers for Solar Cells Obtained by High Throughput Experimentation, *Adv. Energy Mater.*, 2019, **9**, 1900555.

59 W. Chu, W. A. Saidi, J. Zhao and O. V. Prezhdo, Soft Lattice and Defect Covalency Rationalize Tolerance of β-$CsPbI_3$ Perovskite Solar Cells to Native Defects, *Angew. Chem., Int. Ed.*, 2020, **59**, 6435–6441.

60 Y. Wang, X. Liu, T. Zhang, X. Wang, M. Kan, J. Shi and Y. Zhao, The Role of Dimethylammonium Iodide in $CsPbI_3$ Perovskite Fabrication: Additive or Dopant?, *Angew. Chem., Int. Ed.*, 2019, **58**, 16691–16696.

61 C. M. M. Soe, C. C. Stoumpos, B. Harutyunyan, E. F. Manley, L. X. Chen, M. J. Bedzyk, T. J. Marks and M. G. Kanatzidis, Room Temperature Phase Transition in Methylammonium Lead Iodide Perovskite Thin Films Induced by Hydrohalic Acid Additives, *ChemSusChem*, 2016, **9**, 2656–2665.

62 Y. Wei, W. Li, S. Xiang, J. Liu, H. Liu, L. Zhu and H. Chen, Precursor Effects on Methylamine Gas-Induced $CH_3NH_3PbI_3$ Films for Stable Carbon-Based Perovskite Solar Cells, *Sol. Energy*, 2018, **174**, 139–148.

63 W. Ke, I. Spanopoulos, C. C. Stoumpos and M. G. Kanatzidis, Myths and Reality of $HPbI_3$ in Halide Perovskite Solar Cells, *Nat. Commun.*, 2018, **9**, 4785.

64 B. Zhao, S.-F. Jin, S. Huang, N. Liu, J.-Y. Ma, D.-J. Xue, Q. Han, J. Ding, Q.-Q. Ge, Y. Feng and J.-S. Hu, Thermodynamically Stable Orthorhombic γ-$CsPbI_3$ Thin Films for High-Performance Photovoltaics, *J. Am. Chem. Soc.*, 2018, **140**, 11716–11725.

65 K. Wang, Z. Jin, L. Liang, H. Bian, D. Bai, H. Wang, J. Zhang, Q. Wang and S. Liu, All-Inorganic Cesium Lead Iodide Perovskite Solar Cells with Stabilized Efficiency beyond 15%, *Nat. Commun.*, 2018, **9**, 4544.

66 A. Swarnkar, W. J. Mir and A. Nag, Can B-Site Doping or Alloying Improve Thermal- and Phase-Stability of All-Inorganic $CsPbX_3$ (X = Cl, Br, I) Perovskites?, *ACS Energy Lett.*, 2018, **3**, 286–289.

67 Y. Zhou, J. Chen, O. M. Bakr and H.-T. Sun, Metal-Doped Lead Halide Perovskites: Synthesis, Properties, and Optoelectronic Applications, *Chem. Mater.*, 2018, **30**, 6589–6613.

68 W.-J. Yin, Y. Yan and S.-H. Wei, Anomalous Alloy Properties in Mixed Halide Perovskites, *J. Phys. Chem. Lett.*, 2014, **5**, 3625–3631.

69 Z. Yao, Z. Jin, X. Zhang, Q. Wang, H. Zhang, Z. Xu, L. Ding and S. Liu, Pseudohalide (SCN^-)-Doped $CsPbI_3$ for High Performance Solar Cells, *J. Mater. Chem. C*, 2019, **7**, 13736–13742.

70 H. Zhao, J. Xu, S. Zhou, Z. Li, B. Zhang, X. Xia, X. Liu, S. Dai and J. Yao, Preparation of Tortuous 3D γ-$CsPbI_3$ Films at Low Temperature by CaI_2 as Dopant for Highly Efficient Perovskite Solar Cells, *Adv. Funct. Mater.*, 2019, **29**, 1808986.

71 H. Wang, H. Bian, Z. Jin, H. Zhang, L. Liang, J. Wen, Q. Wang, L. Ding and S. F. Liu, Cesium Lead Mixed-Halide Perovskites for Low-Energy Loss Solar Cells with Efficiency beyond 17%, *Chem. Mater.*, 2019, **31**, 6231–6238.

72 K. Wang, Z. Jin, L. Liang, H. Bian, H. Wang, J. Feng, Q. Wang and S. Liu, Chlorine Doping for Black γ-$CsPbI_3$ Solar Cells with Stabilized Efficiency beyond 16%, *Nano Energy*, 2019, **58**, 175–182.

73 M. Jalalah, Y.-H. Ko, F. A. Harraz, M. S. Al-Assiri and J.-G. Park, Enhanced Efficiency and Current Density of Solar Cells *via* Energy-Down-Shift having Energy-Tuning-Effect of Highly UV-Light-Harvesting Mn^{2+}-Doped Quantum Dots, *Nano Energy*, 2017, **33**, 257–265.

74 Q. Wang, X. Zhang, Z. Jin, J. Zhang, Z. Gao, Y. Li and S. Liu, Energy-Down-Shift $CsPbCl_3$:Mn Quantum Dots for Boosting the Efficiency and Stability of Perovskite Solar Cells, *ACS Energy Lett.*, 2017, **2**, 1479–1486.

75 L. Liang, M. Liu, Z. Jin, Q. Wang, H. Wang, H. Bian, F. Shi and S. Liu, Optical Management with Nanoparticles for a Light Conversion Efficiency Enhancement in Inorganic γ-$CsPbI_3$ Solar Cells, *Nano Lett.*, 2019, **19**, 1796–1804.

76 X. Zhang, R. Munir, Z. Xu, Y. Liu, H. Tsai, W. Nie, J. Li, T. Niu, D.-M. Smilgies, M. G. Kanatzidis, A. D. Mohite, K. Zhao, A. Amassian and S. F. Liu, Phase Transition Control for High Performance Ruddlesden-Popper Perovskite Solar Cells, *Adv. Mater.*, 2018, **30**, 1707166.

77 W. Ke, L. Mao, C. C. Stoumpos, J. Hoffman, I. Spanopoulos, A. D. Mohite and M. G. Kanatzidis,

Compositional and Solvent Engineering in Dion–Jacobson 2D Perovskites Boosts Solar Cell Efficiency and Stability, *Adv. Energy Mater.*, 2019, **9**, 1803384.

78 G. Grancini, C. Roldán-Carmona, I. Zimmermann, E. Mosconi, X. Lee, D. Martineau, S. Narbey, F. Oswald, F. De Angelis, M. Graetzel and M. K. Nazeeruddin, One-Year Stable Perovskite Solar Cells by 2D/3D Interface Engineering, *Nat. Commun.*, 2017, **8**, 15684.

79 Q. Wang, Z. Jin, D. Chen, D. Bai, H. Bian, J. Sun, G. Zhu, G. Wang and S. Liu, μ-Graphene Crosslinked $CsPbI_3$ Quantum Dots for High Efficiency Solar Cells with Much Improved Stability, *Adv. Energy Mater.*, 2018, **8**, 1800007.

80 W. Zhu, W. Ma, Y. Su, Z. Chen, X. Chen, Y. Ma, L. Bai, W. Xiao, T. Liu, H. Zhu, X. Liu, H. Liu, X. Liu and Y. Yang, Low-Dose Real-Time X-Ray Imaging with Nontoxic Double Perovskite Scintillators, *Light: Sci. Appl.*, 2020, **9**, 112.

81 Y. Liu, H. Zai, H. Xie, B. Liu, S. Wang, Y. Zhao, D. Niu, H. Huang, Q. Chen and Y. Gao, Effects of $CsPbBr_3$ Nanocrystals Concentration on Electronic Structure And Surface Composition of Perovskite Films, *Org. Electron.*, 2019, **73**, 327–331.

82 K. Wang, Z. Li, F. Zhou, H. Wang, H. Bian, H. Zhang, Q. Wang, Z. Jin, L. Ding and S. F. Liu, Ruddlesden–Popper 2D Component to Stabilize γ-$CsPbI_3$ Perovskite Phase for Stable and Efficient Photovoltaics, *Adv. Energy Mater.*, 2019, **9**, 1902529.

83 H. Wang, S. Xiang, W. Li, H. Liu, L. Zhu, S. Xiao, S. Yang and H. Chen, Skillfully Deflecting the Question: A Small Amount of Piperazine-1,4-Diium Iodide Radically Enhances the Thermal Stability of $CsPbI_3$ Perovskite, *J. Mater. Chem. C*, 2019, **7**, 11757–11763.

84 A. Dutta, S. K. Dutta, S. Das Adhikari and N. Pradhan, Phase-Stable CsPbI3 Nanocrystals: The Reaction Temperature Matters, *Angew. Chem., Int. Ed.*, 2018, **57**, 9083–9087.

85 J. Xi, C. Piao, J. Byeon, J. Yoon, Z. Wu and M. Choi, Rational Core–Shell Design of Open Air Low Temperature In Situ Processable $CsPbI_3$ Quasi-Nanocrystals for Stabilized p-i-n Solar Cells, *Adv. Energy Mater.*, 2019, **9**, 1901787.

86 C. Liu, Y. Yang, X. Xia, Y. Ding, Z. Arain, S. An, X. Liu, R. C. Cristina, S. Dai and M. K. Nazeeruddin, Soft Template-Controlled Growth of High-Quality $CsPbI_3$ Films for Efficient and Stable Solar Cells, *Adv. Energy Mater.*, 2020, **10**, 1903751.

87 C. F. J. Lau, Z. Wang, N. Sakai, J. Zheng, C. H. Liao, M. Green, S. Huang, H. J. Snaith and A. Ho-Baillie, Fabrication of Efficient and Stable $CsPbI_3$ Perovskite Solar Cells through Cation Exchange Process, *Adv. Energy Mater.*, 2019, **9**, 1901685.

88 Z. Li and Z. Jin, HI Hydrolysis-Derived Intermediate as Booster for $CsPbI_3$ Perovskite: from Crystal Structure, Film Fabrication to Device Performance, *J. Semicond.*, 2020, **41**, 051202.

89 Q. Wang, X. Zheng, Y. Deng, J. Zhao, Z. Chen and J. Huang, Stabilizing the α-Phase of $CsPbI_3$ Perovskite by Sulfobetaine Zwitterions in One-Step Spin-Coating Films, *Joule*, 2017, **1**, 371–382.

90 N.-G. Park and K. Zhu, Scalable Fabrication and Coating Methods for Perovskite solar Cells and Solar modules, *Nat. Rev. Mater.*, 2020, **5**, 333–350.

91 J. Gan, J. He, R. L. Z. Hoye, A. Mavlonov, F. Raziq, J. L. MacManus-Driscoll, X. Wu, S. Li, X. Zu, Y. Zhan, X. Zhang and L. Qiao, α-$CsPbI_3$ Colloidal Quantum Dots: Synthesis, Photodynamics, and Photovoltaic Applications, *ACS Energy Lett.*, 2019, **4**, 1308–1320.

92 C. Zuo, A. D. Scully, D. Vak, W. Tan, X. Jiao, C. R. McNeill, D. Angmo, L. Ding and M. Gao, Self-Assembled 2D Perovskite Layers for Efficient Printable Solar Cells, *Adv. Energy Mater.*, 2019, **9**, 1803258.

93 J. M. Ball and A. Petrozza, Defects in Perovskite-Halides and Their Effects in Solar Cells, *Nat. Energy*, 2016, **1**, 16149.

94 D. Zheng, G. Wang, W. Huang, B. Wang, W. Ke, J. L. Logsdon, H. Wang, Z. Wang, W. Zhu, J. Yu, M. R. Wasielewski, M. G. Kanatzidis, T. J. Marks and A. Facchetti, Combustion Synthesized Zinc Oxide Electron-Transport Layers for Efficient and Stable Perovskite Solar Cells, *Adv. Funct. Mater.*, 2019, **29**, 1900265.

95 Z. Wu, Z. Liu, Z. Hu, Z. Hawash, L. Qiu, Y. Jiang, L. K. Ono and Y. Qi, Highly Efficient and Stable Perovskite Solar Cells *via* Modification of Energy Levels at the Perovskite/Carbon Electrode Interface, *Adv. Mater.*, 2019, **31**, 1804284.

96 W. J. Scheideler, N. Rolston, O. Zhao, J. Zhang and R. H. Dauskardt, Rapid Aqueous Spray Fabrication of Robust NiO_x: A Simple and Scalable Platform for Efficient Perovskite Solar Cells, *Adv. Energy Mater.*, 2019, **9**, 1803600.

97 F. Huang, M. Li, P. Siffalovic, G. Cao and J. Tian, From Scalable Solution Fabrication of Perovskite Films towards Commercialization of Solar Cells, *Energy Environ. Sci.*, 2019, **12**, 518–549.

98 A. Ho-Baillie, M. Zhang, C. F. J. Lau, F.-J. Ma and S. Huang, Untapped Potentials of Inorganic Metal Halide Perovskite Solar Cells, *Joule*, 2019, **3**, 938–955.

99 Z. Yu, M. Leilaeioun and Z. Holman, Selecting Tandem Partners for Silicon Solar Cells, *Nat. Energy*, 2016, **1**, 16137.

100 E. L. Unger, L. Kegelmann, K. Suchan, D. Sörell, L. Korte and S. Albrecht, Roadmap and Roadblocks for the Band Gap Tunability of Metal Halide Perovskites, *J. Mater. Chem. A*, 2017, **5**, 11401–11409.